J. exp. Biol. **107**, 21–47 (1983)
Printed in Great Britain © *The Company of Biologists Limited 1983*

WING HAIR PLATES IN CRICKETS: PHYSIOLOGICAL CHARACTERISTICS AND CONNECTIONS WITH STRIDULATORY MOTOR NEURONES

By C. J. H. ELLIOTT*

Max Planck Institut für Verhaltensphysiologie, Abteilung Huber, D-8131 Seewiesen, West Germany

(*Received 14 February 1983–Accepted 23 March 1983*)

SUMMARY

(1) Hairs in the subcostal hair plates of the wings of crickets have a high angular stiffness ($5{\cdot}5\ \mu Nm\ rad^{-1}$) when bent about their base. The mean threshold required to elicit action potentials is 15°. Viscous drag from air movements will not deflect the hairs sufficiently to excite them; this will only occur when the hair is bent by the opposite wing.

(2) The hair sensillae project to the ventral association area of the mesothoracic ganglion, but the endings of the stridulatory motor neurones are all in dorsal or lateral neuropiles of the thoracic ganglia.

(3) Electrical stimulation of the hair plates evokes reliable EPSPs in opener (M99), closer (M90) and wing folding (M85) motor neurones, after latencies of 4–20 ms, depending on the neurone. Properties of the hairs and motor neurones suggest that these EPSPs in the wing folding muscle (M85) and closer (M90) could play an important role in the control of wing position seen in recent behavioural study.

INTRODUCTION

Male field crickets, *Gryllus campestris*, stridulate by rubbing the front wings together, usually holding the right wing over the left (Regen, 1903; Keilbach, 1935; Stärk, 1958; Huber, 1962; Möss, 1971; Elliott & Koch, 1983), although the stridulatory apparatuses on both sides appear to be mirror images (Stärk, 1958). In males induced to stridulate in the inverted orientation of the front wings, almost no sound is produced, at least immediately after inversion. What little there is, sounds scratchy and is certainly not attractive to conspecifics (Huber, 1962; Elliott & Koch, 1983).

Normally the intact singing male threequarters opens the wings at the end of the opening stroke. The wing movements are limited so that, when seen from above, no 'gap' appears between the opened wings; such a gap would be a prerequisite for the inversion to left over right singing.

There are two hair plates on each wing adjacent to the file and plectrum: one on the dorsal surface and the other ventrally (Regen, 1903). Each hair plate contains some

* Present address: School of Biological Sciences, The University of Sussex, Falmer, Brighton, BN1 9QG, U.K.

Key words: Cricket stridulation, hair plate, motor neurone.

50 mechanoreceptive hairs, those on the underside being longer (~250 μm) than those in the upper plate (~120 μm) (Elliott, Koch, Schäffner & Huber, 1982). Wing position is destabilized by covering all four hair plates with nail varnish (Möss, 1971), destruction of all the hairs individually (Elliott & Koch, 1983), or cutting off the parts of the wings with the hair plates (Regen, 1903). This sometimes leads to an inversion of the wings.

As previously reported (Elliott *et al.* 1982), electrical stimulation of the hair plates evokes EPSPs in motor neurones of stridulatory muscles and it was suggested that these short latency, reliable synaptic events could be part of the control mechanism.

The first aim of this paper is the description of the mechanical and physiological characteristics of the mechanosensitive hairs and their connections to stridulatory motor neurones. Secondly, the extent to which the neural observations can account for the behavioural results of Elliott & Koch (1983) will be considered in the Discussion.

MATERIALS AND METHODS

Crickets

Male *Gryllus campestris* were used in all experiments, either caught as last instar nymphs or adults from the region of Meran (Italy) or the Kaiserstuhl (West Germany) or out of cultures raised in Seewiesen (up to the third generation from wild caught crickets).

Measurement of the stiffness of the hairs

To obtain absolute values for the static stiffness of the hairs, they were deflected by a microelectrode of known stiffness and the deflection of hair and microelectrode measured (cf. Wiese, 1976). From these deflections and the stiffness of the electrode, the stiffness of the hair can be calculated.

The stiffness of a long thin glass microelectrode was determined by suspending short lengths of 50 μm diameter platinum wire of known weight on the tip and measuring the deflection. The stiffness (S_e) is then the slope of the graph of force against deflection.

The hair was bent with a microelectrode as follows: the anal part of the wing was cut off and mounted on Plasticene on a rotating stage so that the selected hair was vertical and in the centre of the field of view of a compound microscope fitted with a measuring ocular. The microelectrode was mounted on a piezoelectric device, to produce horizontal movement of the electrode tip (Fig. 1). For a given voltage applied to the device, the distance moved when the tip was moving freely was greater than the distance (d) moved when the tip was in contact with the hair. The difference in the displacements (x) was then the deformation of the electrode due to the hair and so the force, F, applied to the electrode was:

$$F = S_e x.$$

By Newton's law this was also the force applied to the hair which moved the tip of the hair the distance d. Hence, the stiffness of the hair, S_h was:

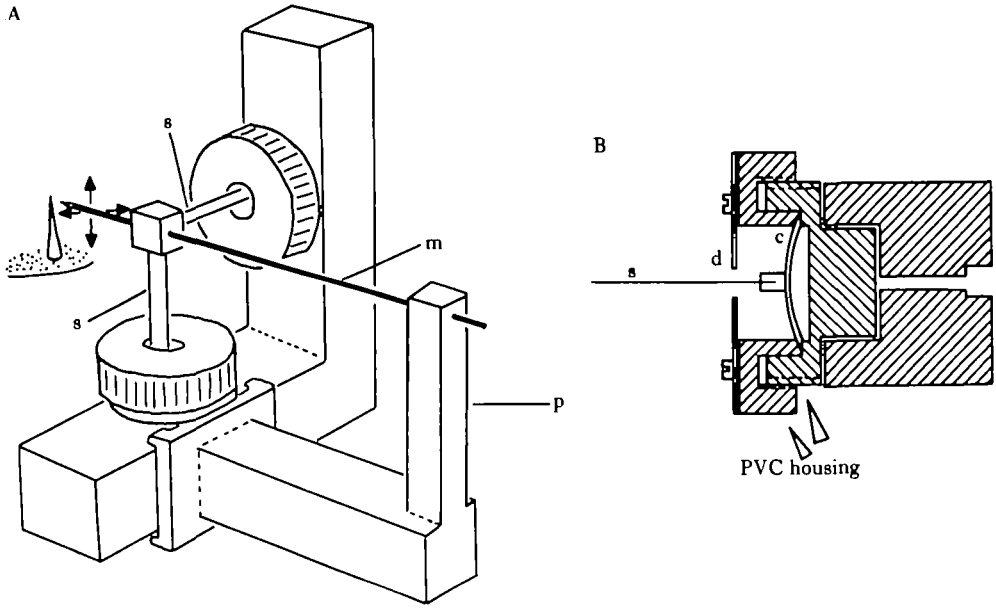

Fig. 1. Apparatus used to provide controlled movement of microelectrodes to bend hairs. The blunt end of the electrode is held fixed in a Perspex block (p) in the brass mainframe, while the sharp end is mounted in a small Perspex block glued to the end of two strips of spring steel (s). Each steel strip is mounted on the centre of a 23 mm diameter piezoelectric crystal (Motorola). (A) Schematic diagram of the apparatus showing how the hair is brought up to the microelectrode (m). (The hair is shown on a much larger scale.) The microscope is omitted for clarity. The arrows show the directions of movement when voltages (up to ±70 V) are applied to one of the crystals. (B) Cross section through the centre of one of the crystals, showing the way the crystal (c) is held in its PVC housing on the brass mainframe. The steel strip (s) is glued into the Perspex block mounted centrally on the crystal. Over the PVC housing lies a thin brass disc (d). The disc, steel strip and brass mainframe are all earthed.

$$S_h = \frac{F}{d} = \frac{S_e x}{d}.$$

Electrodes were pulled so that x and d were of the same order of magnitude to help minimize the errors. Such electrodes had stiffnesses, $S_e = 100\ N\ m^{-1}$. By rotating the stage holding the hairs, their stiffness could be measured in different directions.

Neurophysiological response of single hair sensillae to displacement

The piezoelectric driver described in the last section was used to deflect the hairs while their neural response was recorded. Stiff microelectrodes were pulled and filled with saline solution (Bishop & O'Shea, 1982) to which polyvinylpyrrolidon (PVP), $0{\cdot}2\ g\ ml^{-1}$, had been added to ensure a stable recording (Kaissling & Thorson, 1980). The microelectrode was surrounded by a braid, driven to the same potential as the interior of the electrode from a voltage follower circuit built to the design of U. T. Koch (FB Biologie 13/566, Universität, D-6750 Kaiserslautern, W. Germany) using LF 356 integrated circuits.

A male cricket was firmly mounted on a moving stage in a Plasticene block with the hair horizontal and the tip of the hair was cut off with a small pair of pincers (see Elliott & Koch, 1983). The end of the remaining stump was inserted into the end of the

electrode by moving the stage. Good contact, which was indicated by a drop in resistance, was usually established by dipping the tip of the electrode into salin without PVP for a minute before bringing hair and electrode into contact.

The signal from the microelectrode was amplified by a d.c. coupled amplifier (U. T. Koch) and recorded at low gain on one channel of a Racal 7DS tape recorder ($3\frac{3}{4}$ ips). The signal was filtered from 0·1 to 1·0 kHz and recorded at higher gain. Also tape-recorded were the driving signals applied to both crystals.

Electrical stimulation of whole hair plates

To stimulate the hair plates electrically, the ends of the hairs in both upper and lower plates were cut off with the pincers. A vaseline cup was constructed around the cut ends – one on the upper and one on the lower surfaces of the wing – and filled with saline. One stimulating electrode was inserted into each cup. The stimulus duration was kept as short as possible to allow accurate timing of response latencies, and so high stimulus voltages were used.

The axons of the hairs run in N1C: their activity in response to the electrical stimulation was recorded with hook electrodes of 100 μm silver wire, insulated with a mixture of vaseline and mineral oil. The electrodes were placed just above the junction of N1C and N1D.

In each preparation a compound action potential was recorded in N1C 1·5–6 ms after electrical stimulation of the hair plates. This increased in size with stimulus strength but was only present if the ends of the hairs had been cut through. Very large (>75 V) stimuli to the hair plates induced other, slower, responses in N1C. If N1C was stimulated, and the electrodes in the vaseline cups over the hairs used for recording, then compound potentials were recorded after a short latency (less than 6 ms). These electrophysiological experiments suggest that the short latency response is due to stimulation of the hair plate neurones. Transmission and scanning electron microscope examination (K.-H. Schäffner, personal communication) show that hairs are the only sensory sensillae present in this region of the wing.

Electromyograms were made with electrodes of 50 μm copper wire, insulated, but for the tip, with lacquer. These were inserted into the stridulatory muscles under a dissecting microscope.

Staining of the projections of neurones within the thoracic ganglia with cobalt

Where the projections of whole nerves were to be examined the male cricket was dissected from the dorsal side and the cut end of the nerve placed in a small vaseline cup containing a cobalt solution, for at least 12 h at 4 °C (Altman & Tyrer, 1980). Cobalt chloride, cobalt nitrate, cobalt-proline and cobalt-lysine complexes (Gallyas, Lénárd & Lazar, 1978) were all used. The solution used and running time are given in the figure legends. To stain motor neurones to a particular part of a muscle, the nerve was teased out from among the fibres by gently stroking along the length of the muscle fibres with sharp forceps and only the part which had been inside the muscle was placed in the cup.

To examine the projections of the hair plates selectively, the hairs were cut through with the pincers and a vaseline cup constructed over the stumps.

After the cobalt had run into the CNS, it was precipitated with ammonium sulphide

in saline (Tyrer & Altman, 1974), washed in clean saline and fixed in Carnoy's fluid for 1 h. Some ganglia were fixed for 1 h in alcoholic Bouin's instead; after fixation the picric acid was removed by two changes of 10 % ammonium acetate in 70 % alcohol. The cobalt sulphide precipitate was intensified using the method of Bacon & Altman (1977), but the developer base contained only 3 % sucrose.

Intracellular recording and staining

Microelectrodes pulled from thick-walled glass were filled with a 3 % solution of Lucifer Yellow CH in 1 M lithium chloride and had a resistance of 50–80 MΩ. The male cricket was dissected from the dorsal side under saline (Bishop & O'Shea, 1982). The electrodes were tapped into the integrating segments of the motor neurones using the method of Wohlers & Huber (1978) and Pearson & Fourtner (1975) without the use of protease. Motor neurones were identified both by the correspondence of intracellular spikes with EJPs in the muscles and visually.

Neurones were stained by passing 500 ms pulses of hyperpolarizing current (3–5 nA) at 1 Hz. Blocking of the electrode was prevented by occasionally reversing the polarity of the current. Cells were well stained after 5–10 min. The synaptic response to stimulation of the hair plates was unaffected by injection of the dye. Ganglia were fixed according to Stewart (1978) and photographed as whole mounts in methyl salicylate. Neurones were reconstructed from slides made on High Speed Ektachrome.

RESULTS

The mechanical and electrical properties of the hairs

When a maintained force was applied to the tip of one of the hairs in a ventral hair plate, in the direction of the file, the mean ratio of the force/deflection of the tip was 88 N m^{-1} (S.E.: 25 N m^{-1}, $N = 4$). Observation of the hair through a compound microscope showed that the hair was rigid and that all the bending occurred at the insertion of the hair. Angular stiffness is defined as the torque needed to deflect the hair by one radian. The angular stiffness was therefore 5·5 μNm rad^{-1}.

The stiffness remained constant over the measured range of ±1 to ±4 degrees deflection (Spearman rank correlation test: $r_s = -0{\cdot}27$, $N = 11$, N.S., $P >> 5$ %). The hairs were not equally stiff in all directions, the ratio of maximum to minimum stiffness ranging from 2 to 7. Hairs could be more easily bent towards and away from the file (Fig. 2), as occurs in stridulation. The most likely explanation for the asymmetry in the stiffness is that most – but not all – of the hairs insert into the cuticle at an angle of about 70° and not perpendicularly. Most hairs point towards the mirror cell (K.-H. Schäffner & C. J. H. Elliott, unpublished results). This explanation is supported by the fact that for the two most asymmetrical hairs this is the direction of maximum stiffness. It should be noted that Nicklaus (1965) and Camhi (1969), who examined cercal hairs of *Periplaneta* and head hairs of *Schistocerca* respectively, attributed their asymmetry in stiffness to elliptical sockets. This can not explain the asymmetry in the wing hairs because removal of these hairs leaves circular sockets (K.-H. Schäffner & C. J. H. Elliott, unpublished results).

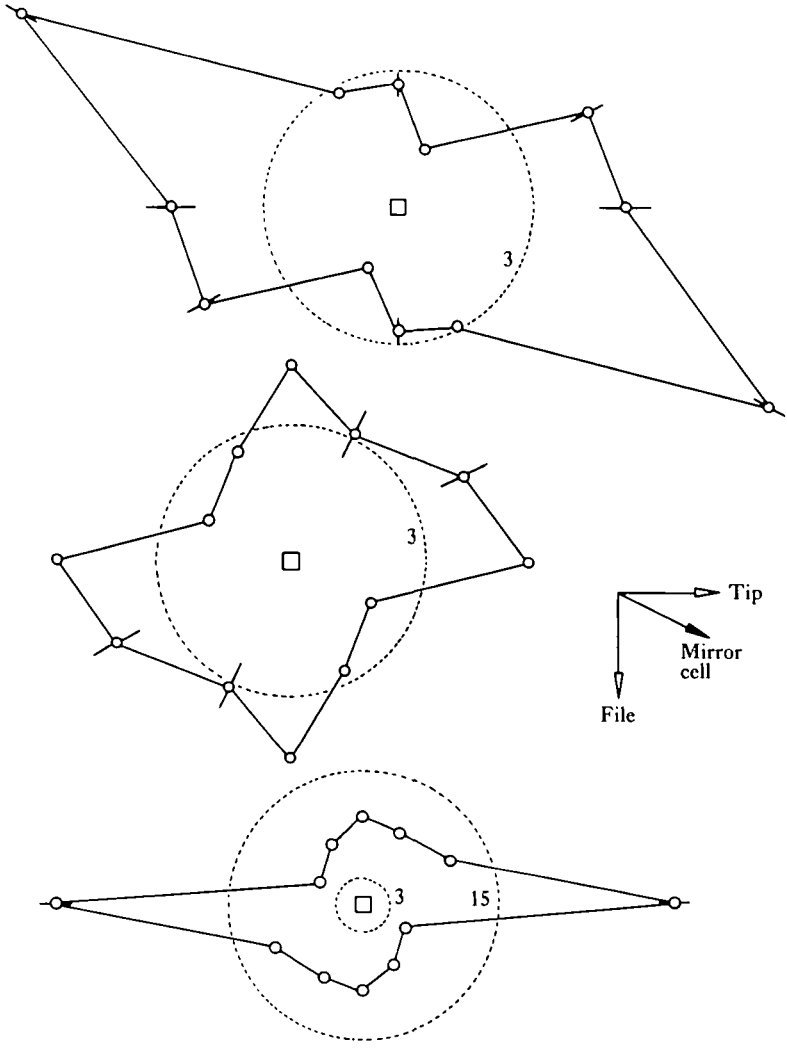

Fig. 2. Polar plot of the static stiffness of three hairs from ventral hair plates. The dotted lines indicate angular stiffnesses of 3 and 15 μNm rad^{-1} respectively. For the third hair the scale is reduced. In each direction, at least three measurements were made, so that the points are means and the bars standard errors. The measurements are symmetrical about the resting position (square) because the driving voltage applied to the piezoelectric crystal was a sinusoid (0·1 Hz) about the resting position.

When a hair was deflected sufficiently in any direction, then a negative-going receptor potential was recorded. In the example shown in Fig. 3, a larger receptor potential was recorded for a negative driving voltage than for a positive one. The largest potential was recorded slightly before the maximum displacement was reached. The receptor potential gave rise to action potentials which were recorded as electrotonically propagated remnants, 0·5–2 mV in size, (depending on the preparation). As the amplitude of the stimulus was increased, so did the receptor potential and the number of action potentials evoked. At high intensities, spikes could be recorded at two different parts of the cycle: just before maximum displacement in both positive and negative directions. When the stimulus intensity was sufficient to

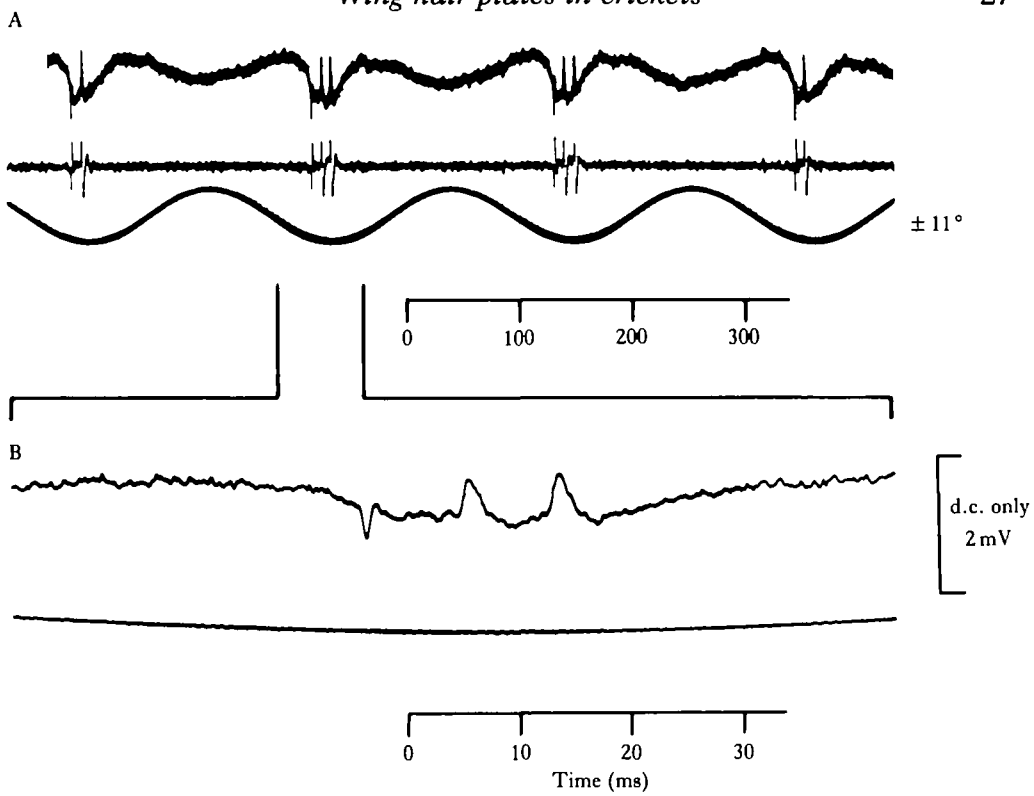

Fig. 3. Neural response of a hair in the dorsal hair plate to sinusoidal stimulation of 11° about the resting position. The upper record (A) shows the applied stimulus (lower trace) and the response – both d.c. (upper trace) and a.c. (middle trace) coupled. Part of the record is shown below on an expanded time scale (B): here the a.c. coupled trace is omitted. Note the two different spike shapes.

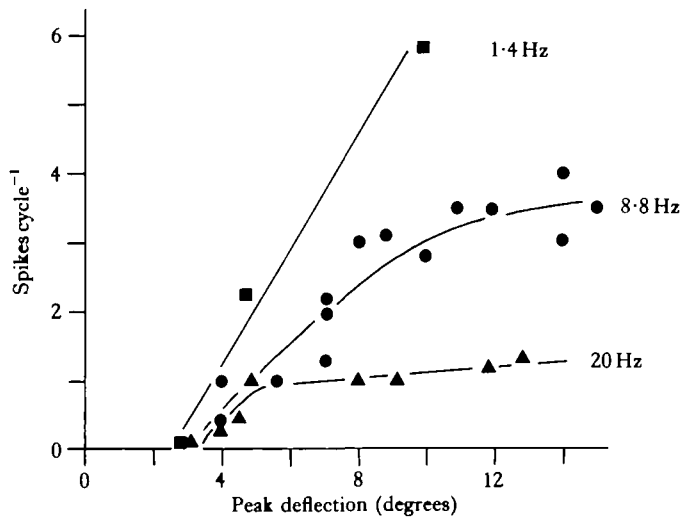

Fig. 4. Neural response of a ventral hair plate sensilla to mechanical stimulation at 1·4 Hz (squares), 8·8 Hz (circles) and 20 Hz (triangles). The graph shows the response (spikes cycle^{-1}) to sinusoidal stimuli of slowly varying amplitude about the resting position.

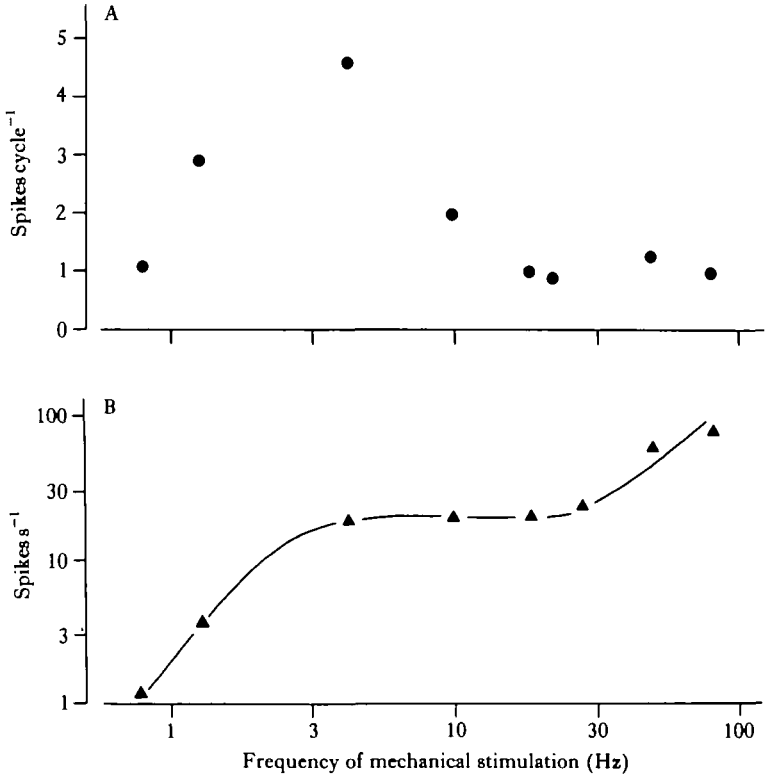

Fig. 5. Neural response of a second ventral hair plate sensilla to a constant amplitude of mechanical stimulation about the resting position at frequencies of 0·8–80 Hz. The response is shown both as (A) gain (spikes cycle^{-1}) and also (B) mean firing rate (spikes s^{-1} = spikes cycle^{-1} × stimulus frequency).

generate more than one action potential per cycle, the first action potential in each group differed from the others. The first potential always started with a more pronounced negative phase, while its positive phase was smaller and of shorter duration (Fig. 3B). As the stimulus intensity was then lowered, spikes dropped out. When only one spike remained per cycle, its shape corresponded with that of the first in each group.

Figs 4 and 5 show the sensitivity of hairs from the lower hair plate to sinusoidal stimuli of different frequencies and amplitudes. The threshold was constant at all frequencies in the range 1 to 50 Hz. At high frequencies, a small increase in stimulus amplitude evoked one spike regularly in each cycle. A further increase in amplitude, however, evoked no increase in the number of action potentials (Fig. 4, 20 Hz). At

Fig. 6. Cobalt staining of the axons of the hair sensillae to the mesothoracic ganglion. (A) Whole upper hair plate stained: dorsal view. (B) A second preparation with the whole upper plate stained, but only the projection of a single hair drawn from a dorsal view. (C) The whole lower hair plate stained: transverse section of the mesothoracic ganglion. (i) Whole ganglion showing the ventral association area (VAC; dotted outline) and areas in which the endings are densest in two successive 40 μm sections at the level of nerve 3. (ii) Part of the ganglion at higher magnification, showing the endings in one 40 μm section at the level of nerve 3. All preparations made with cobalt-proline or cobalt-lysine complexes; running time 48 h.

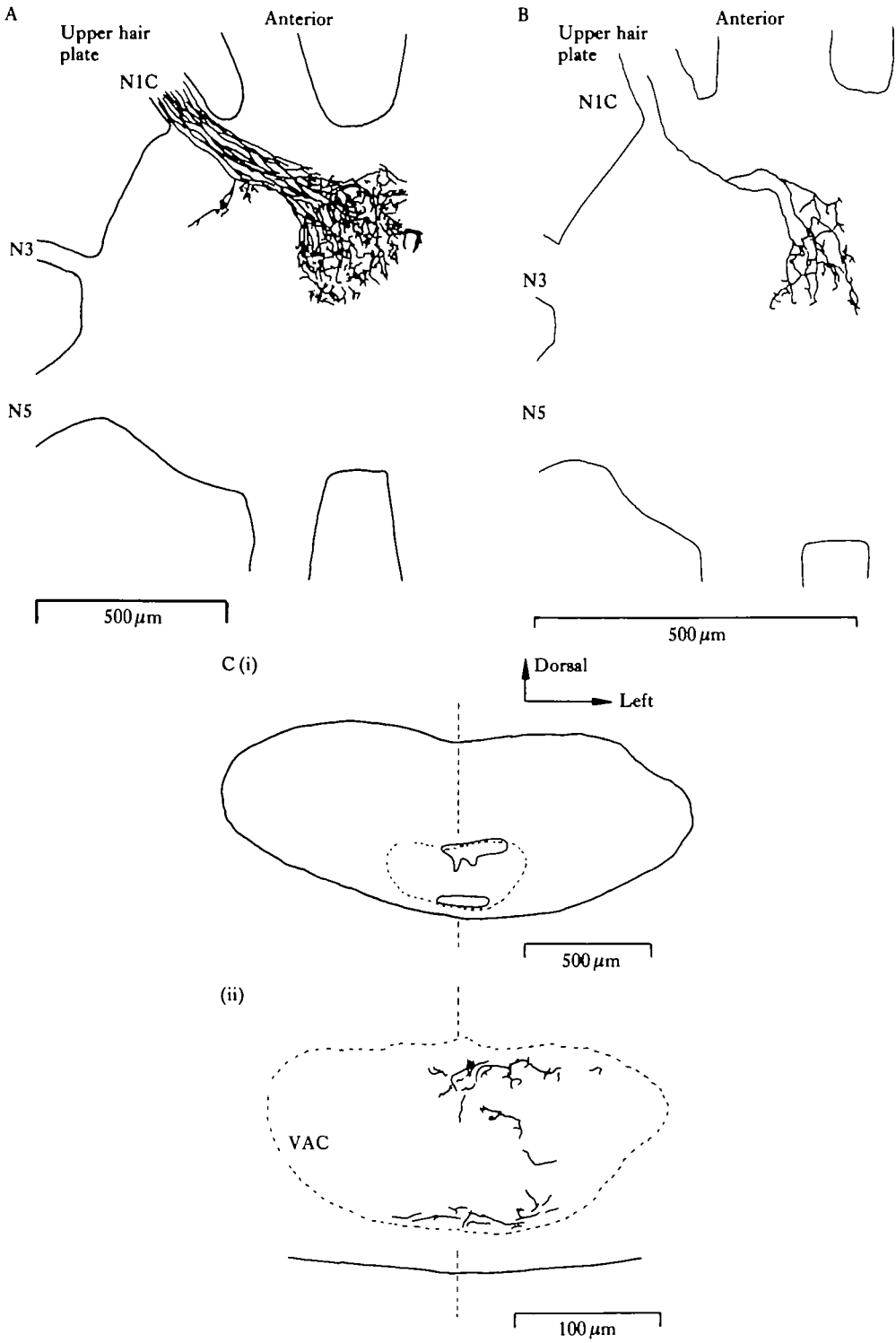
A
Upper hair plate
Anterior
N1C
N3
N5
500 μm
B
Upper hair plate
Anterior
N1C
N3
N5
500 μm
C (i)
Dorsal
Left
500 μm
(ii)
VAC
100 μm

Fig. 6A–C

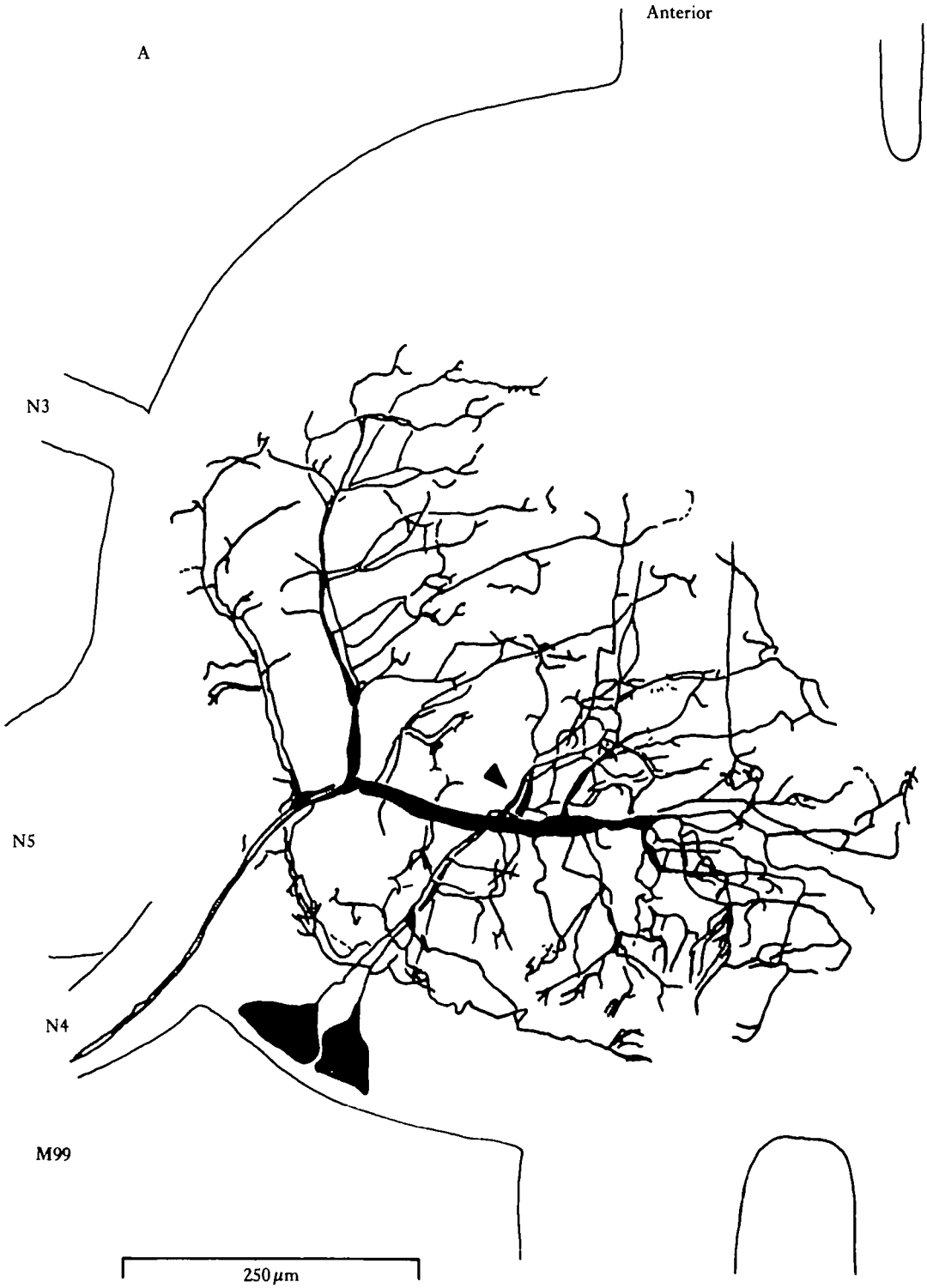

Fig. 7A

low frequencies, the number of spikes per cycle increased linearly with stimulus amplitude (Fig. 4, 1·4 Hz) while at intermediate frequencies the number of spikes increased at first, but soon reached a plateau (Fig. 4, 8·8 Hz). Thus it would appear that the response of the hair sensillae at the higher frequencies is restricted by the refractory period of the neurone. Results from a second hair are shown in Fig. 5A, where the response to a constant amplitude of stimulus over a wider range of frequencies is presented. The peak gain (spikes cycle^{-1}) lay between 1 and 3 Hz and fell off at higher frequencies to a fixed 1 spike cycle^{-1}. This was typical of all hairs examined. At frequencies below 3 Hz, the gain also decreased. The rate of decline varied between hairs: in some the response at 0·1 Hz was 70 % of that at the peak, but in others the response was already small at 0·8 Hz (Fig. 5A). The mean rate of action potentials (the product of gain and stimulus frequency) was constant at 20 spikes s^{-1} for stimulus frequencies between 3 and 30 Hz (Fig. 5B). Above this frequency, the mean rate rose rapidly. For stimuli at less than 3 Hz, the mean rate dropped off with decreasing frequency; the rate of decline depending on the gain characteristics of the particular hair.

No difference was found between the characteristics of the neural response of the hairs in the upper and lower hair plates. For sinusoidal stimulation parallel to the file

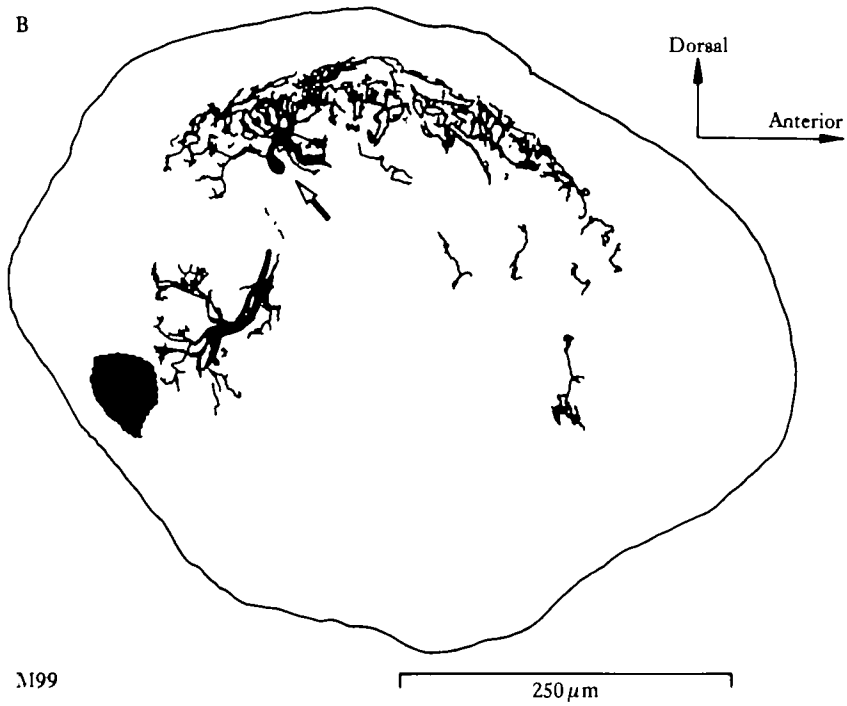

Fig. 7. Projections of the two motor neurones from M99 (opener) to the mesothoracic ganglion. (A) The principal branches of both neurones in dorsal view. (M99 is only innervated by two axons, Elepfandt, 1980). One neurone (indicated in black) has a branch (arrow) that projects to a layer more central than any occupied by the other neurone. (3 % cobalt nitrate for 20 h.) (B) Sagittal section (40 μm) just medial to the cell bodies. The position of the cell bodies – present in the next section – is indicated in grey. The arrow points to the integrating segments, dorsally located in the ganglion. Note that the neurites which run between the cell bodies and the integrating segment give off many branches; this is typical of the cricket wing-moving motor neurones. (Cobalt-lysine complex for 20 h.)

– the direction in which the hairs would be bent back and forth during stridulation – the mean threshold was 15·5°, peak to peak. When bent in other directions the threshold was unchanged.

The projections of the hair sensillae

The axons from the hair sensillae in both dorsal and ventral hair plates run alongside the second anal vein (Comstock & Needham, 1899) (= XI of Voss, 1904) to the base of the wing. Here the three branches of the wing nerve fuse together forming N1C of the mesothoracic ganglion. The axons enter the ganglion and run ventrally towards the dense neuropilar region, called the ventral association area (VAC) (Zawarzin, 1924; Tyrer & Gregory, 1982) (Fig. 6). A few axons give off small retrograde twigs before reaching the VAC; the twigs terminate within 150 μm. The axons from hairs in both the upper and lower hair plates terminate within the VAC in numerous small branches, some crossing the midline. Most of the terminations are in two groups; one just at the dorsal edge of the VAC, and the other, with fewer endings near the ventral limit of the VAC (Fig. 6C).

The detailed morphology of motor neurones to stridulatory muscles

The location and innervation of the muscles used to move the wings is described in detail by Kutsch & Huber (1970). The projection of muscles, M59, 81a and b, 83, 85, 89a, 90, 91, 97, 98, 99, 103a and b and 117 in the thoracic ganglia have all been established. M99 (subalar) is the most important opening muscle during stridulation. This muscle is supplied by N4D of the mesothoracic ganglion. This nerve also innervates two other important stridulatory muscles: M90 (remotor coxae) – active in the

Fig. 8. Projections of M90 (closer) motor neurones in the mesothoracic ganglion. (A) Whole nerve (9 axons, Elepfandt, 1980) stained; dorsal view. Nine cell bodies are found: one large one anteriorly (*A*), three large (*B*, *C*, *D*) and one small (*E*) posteriorly, just lateral to the connectives and four DUM cells between the connectives (only one DUM cell is indicated). The DUM cells appear to supply both left and right M90, because when both these muscles are back-filled, the number of DUM cells filled is still four. The dashed line encloses all the endings of the motor neurones, and the dotted line the dorsal-most endings on either side of the lateral dorsal tract. The DUM cells however branch anteriorly from the ends of the two short horns indicated. (1 % cobalt nitrate for 20 h.) (B) Transverse section (40 μm) at the posterior edge of N3 of a second preparation in which the whole nerve is stained. This shows the branching of the neurones in a layer just below the sheath. The branching is most intense dorsally, but is also extensive in the lateral regions, some of the branches being almost ventral. The arrow indicates the neurite of the anterior motor neurone (*A*). (3 % cobalt chloride for 20 h.) Scale bar = 250 μm. (C) The pattern of primary branching is characteristic of each motor neurone. (i) Cell *A*. This cell has an anteriorly located cell body. Two kinds of twigs are present: those arising from the first two primary branches from the integrating segment and from the neurite are all in the lower regions of the ganglion, in lateral or posterior neuropiles, just under the sheath. They also appear thicker than the twigs on the other primary branches which are all in the dorsal most layers of the ganglion. Unlike the other M90 motor neurones, none of the branches of cell *A* extend medial to the lateral dorsal tract. The open circles indicate the course of the integrating segment and neurite of cell *D*. The dashed line encloses the endings of all M90 motor neurones. The positions of the other cell bodies are indicated in outline. (Cobalt-lysine complex for 20 h, whole nerve stained and cell *A* drawn with camera lucida.) (ii) Cell *B*. Characteristic of this cell is the straight integrating segment, with two thick branches projecting anteriorly at least as far as the level of nerve 3. This cell supplies the most lateral parts of M90 only (Lucifer Yellow fill). (iii) Cell *C*, which supplies the dorsal part of M90, also has a posteriorly located cell body. Unlike the cell *B*, the integrating segment of this cell (*C*) curls round posteriorly. (Cell *D* has a similar curling integrating segment, but the first and second major anterior branches are equal in length.) (Nerve to the dorsal part of M90 filled with 1 % cobalt nitrate for 20 h.)

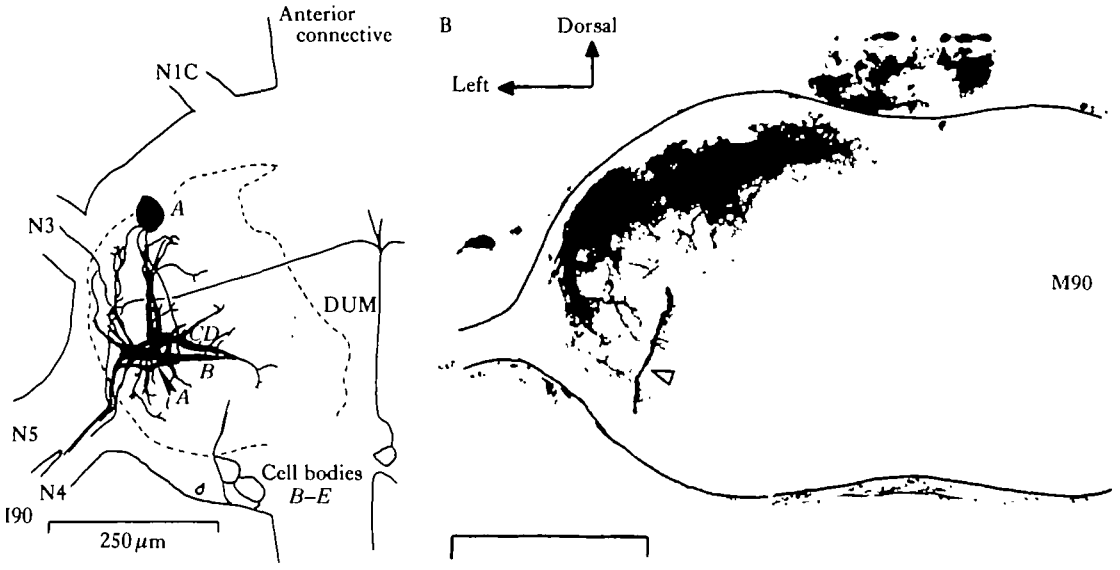
Anterior connective
N1C
N3
A
DUM
CD
B
A
N5
N4
I90
Cell bodies B–E
250 μm
B
Dorsal
Left
M90

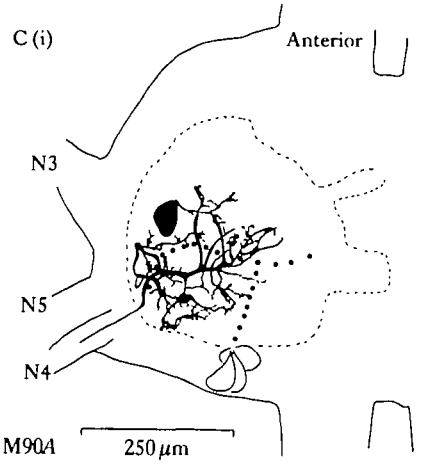
C (i)
Anterior
N3
N5
N4
M90A
250 μm

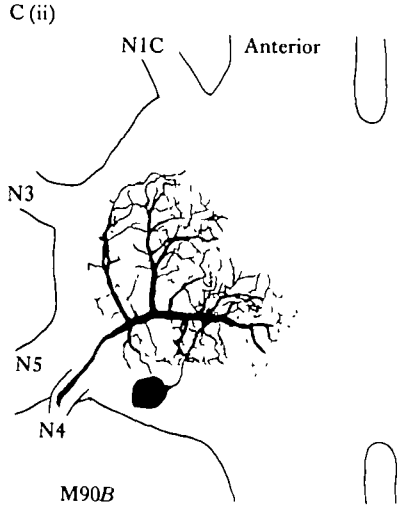
C (ii)
N1C
Anterior
N3
N5
N4
M90B

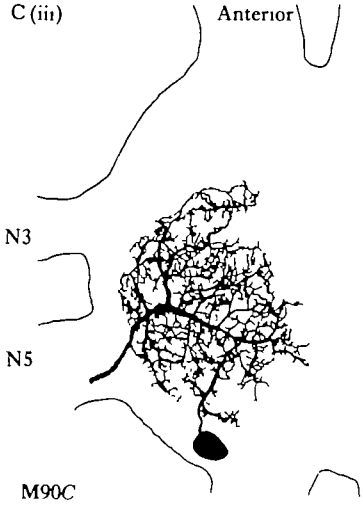
C (iii)
Anterior
N3
N5
M90C

(*Facing p. 32*)

Fig. 10. Photomicrographs of 40 μm sections near the entry of N3 showing projections of the motor neurones to the first and second basalar muscles. (A) M97 (first basalar); 3 % cobalt nitrate for 20 h. (B) M98 (second basalar); 3 % cobalt nitrate for 20 h. Of these two muscles, which are both openers, only M98 (second basalar) is active during stridulation (Kutsch, 1969). The motor neurones for both muscles branch in the same dorsal neuropile. M98 also shows branches in the lateral neuropile. This is, however, invaded by other non-stridulatory motor neurones. Each of the wing muscles branch within these neuropiles [c.f. Fig. 8B, showing M90 (closer) projections]. Scale bar = 250 μm.

closing stroke – and M85 (tergopleural), or wing folding, muscle which is tonically active during stridulation. These three muscles are the most intensively studied, because, although they have diverse functions, their innervation is through branches of N4D.

For this reason, their branching patterns within the mesothoracic ganglion are presented here in detail (M99: Fig. 7; M90: Fig. 8; M85: Fig. 9). The projection of the other muscles to this ganglion are indicated in Figs 10 to 14. The detailed anatomy may be summarized as follows:

(1) All the terminals of the motor neurones are dorsal or lateral, not far under the sheath. Except for muscles 81 and 85 all projections are ipsilateral.

(2) Left and right motor neurones are mirror images of each other, at least at the level of the primary branches.

(3) The somata of the motor neurones in the mesothoracic ganglion are mostly laterally located, just under the sheath of the ganglion. Most of the cell bodies for N1 are contralateral, between N1 and N2; those supplied from N3 and N4 have mostly ipsilateral cell bodies next to the anterior and posterior connectives respectively.

(4) The neurites of these motor neurones do not run directly from cell body to integrating segment unbranched, but give rise to branches (cf. locusts Burrows, 1973; Tyrer & Altman, 1974).

(5) The most dorsal terminations of the motor neurones are interrupted by the lateral dorsal tract. On both sides of this tract many of the fine branches run anteriorly or posteriorly parallel to the tract, perhaps making serial synapses with the neurones in it.

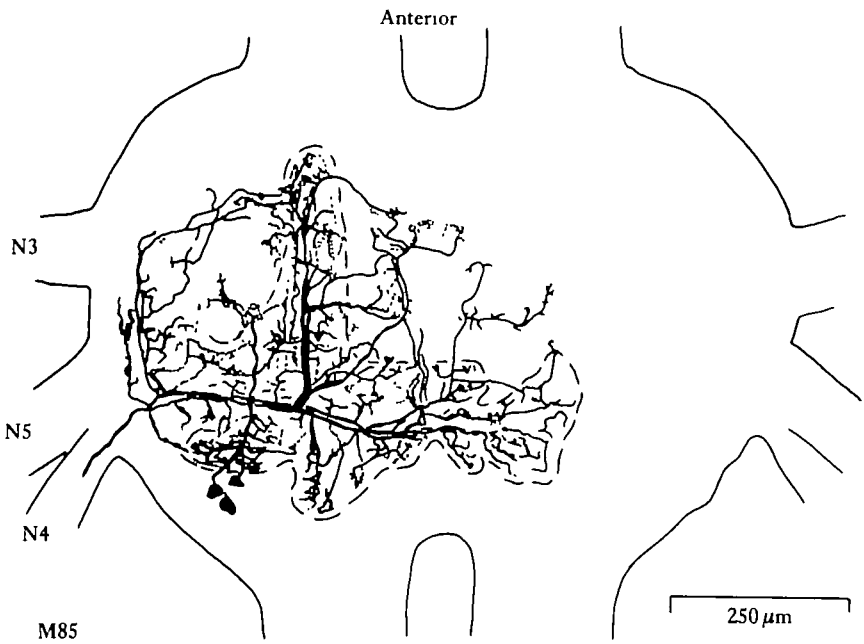

Fig. 9. Motor neurones to M85, wing folding muscle dorsal view. Three neurones filled, each crossing the midline. The dashed line contains the regions of densest endings (1 % cobalt nitrate for 20 h).

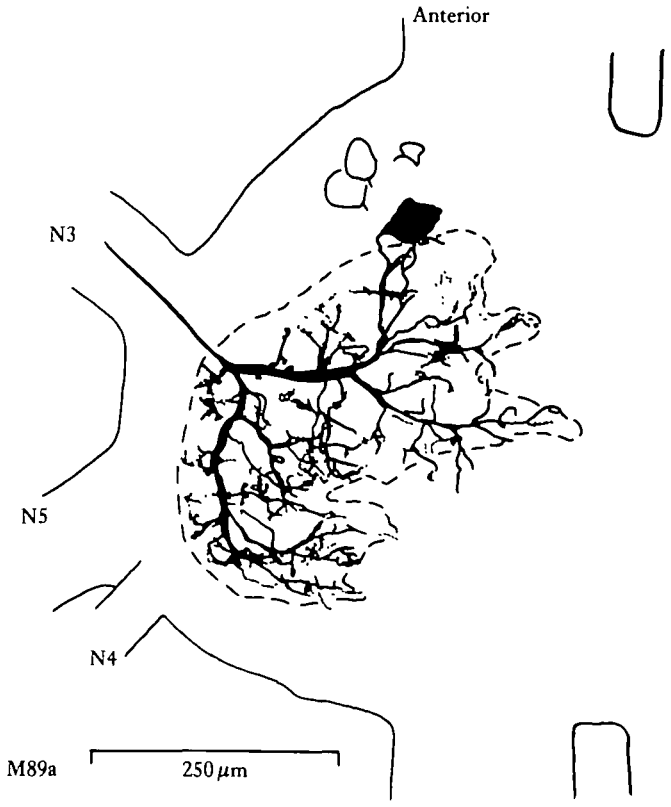

Fig. 11. The projection of M89a (closer) motor neurones to the mesothoracic ganglion. Drawing of a dorsal view. The projection of one of the three large cells is shown; the position of the other three cell bodies is indicated in outline. The endings of all four motor neurones lie within the dashed line (cobalt-lysine complex for 20 h). More strongly stained preparations reveal DUM cells with somata posteriorly between the connectives. They have axons in both ipsi- and contralateral N3 and N4.

(6) All the muscles are supplied by more than one motor neurone. For each of the muscles studied in detail (M90, M99 and M85) the motor neurones for any one muscle can all be distinguished from each other by the characteristics of the primary branching pattern. Stimulation of individual, morphologically identified, motor neurones by intracellular injection of current shows that each motor neurone supplies a fixed part of the muscle (cf. innervation of M99 in *Schistocerca*, Kutsch & Usherwood, 1970).

(7) No consistent pattern of difference has been found between the tracts and neuropiles occupied by opener and closer motor neurones (cf. for example 90 and 99), nor between those used in singing and those used only in other types of behaviour (cf. for example 97 and 98).

(8) Some of the muscles are also innervated by DUM cells: their cell bodies are posteriorly located on the midline between the connectives. These neurones always serve more than one muscle and are usually symmetrical: this is not the case for the two DUM neurones for M81 (dorsal longitudinal muscle) (Fig. 13B) (cf. locusts, Altman & Tyrer, 1977). Not every muscle has a DUM cell, however: for example there is none for M99.

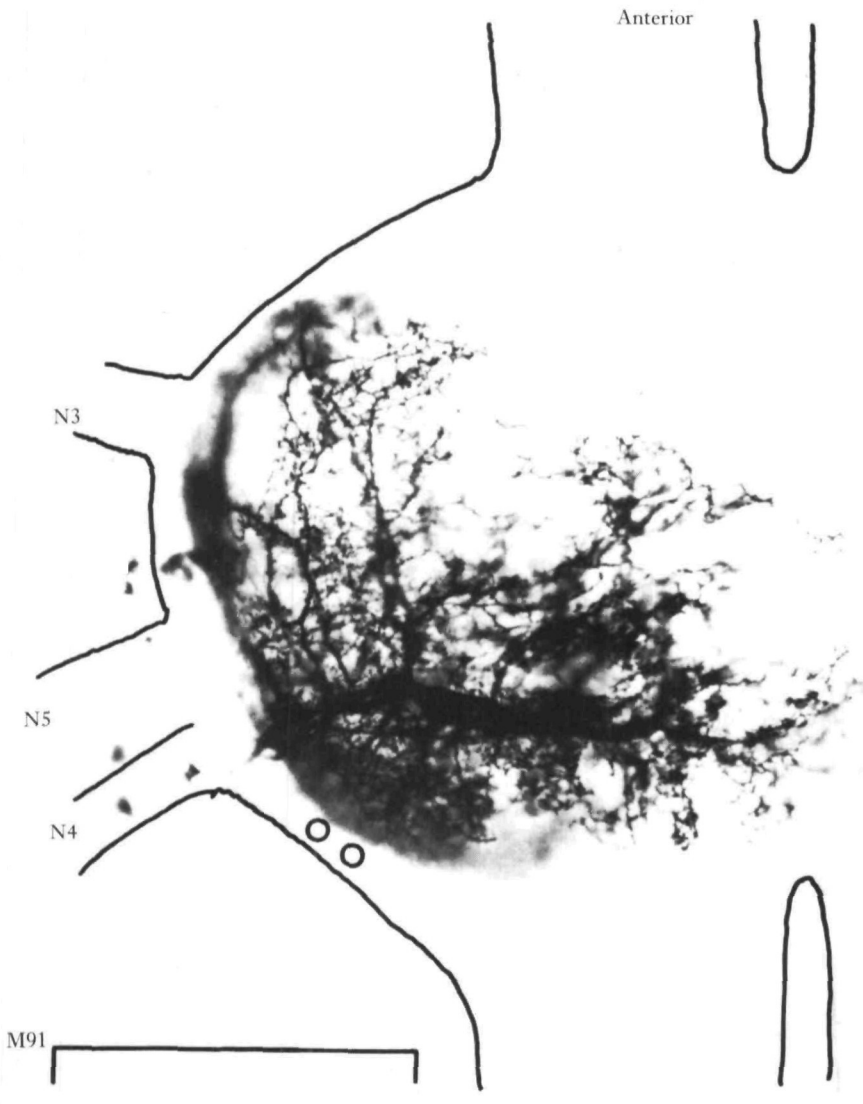

Fig. 12. Photomicrograph of the projection of M91 (closer) motor neurones to the mesothoracic ganglion, dorsal view. The cell bodies lie out of the plane of focus, but their positions are indicated by the open circles. The shape of the branches of these motor neurones is different from that of the other N4D motor neurones (N4D supplies M85, M90, M91 and M99). Scale bar = 250 μm.

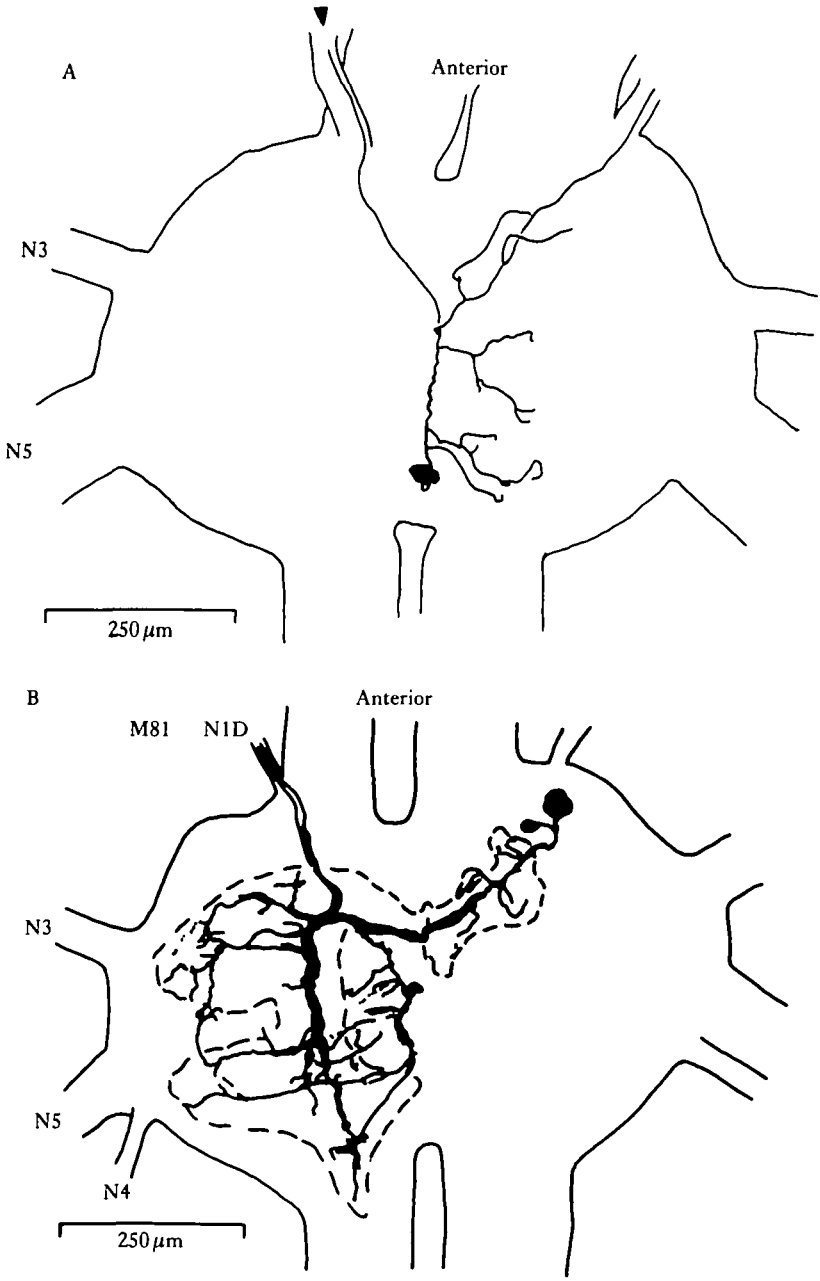

Fig. 13. Projections of M81 motor neurones to the mesothoracic ganglion. M81 is the dorsal longitudinal muscle and is supplied by N1D. (A) A neurone with its cell body in the DUM cluster and axons in both left and right N1D. Note that – unlike the DUM cells with axons in N3 and N4 – this cell has asymmetrical branches. Well stained preparations usually revealed a second DUM cell. (B) Three motor neurones; two with anterior contralateral cell bodies and one ventrally on the midline. The dashed line encloses the areas with a high density of endings. Both drawings of the same whole mount, 3% cobalt nitrate for 20 h. (At least four motor neurones are also stained in the prothoracic ganglion.)

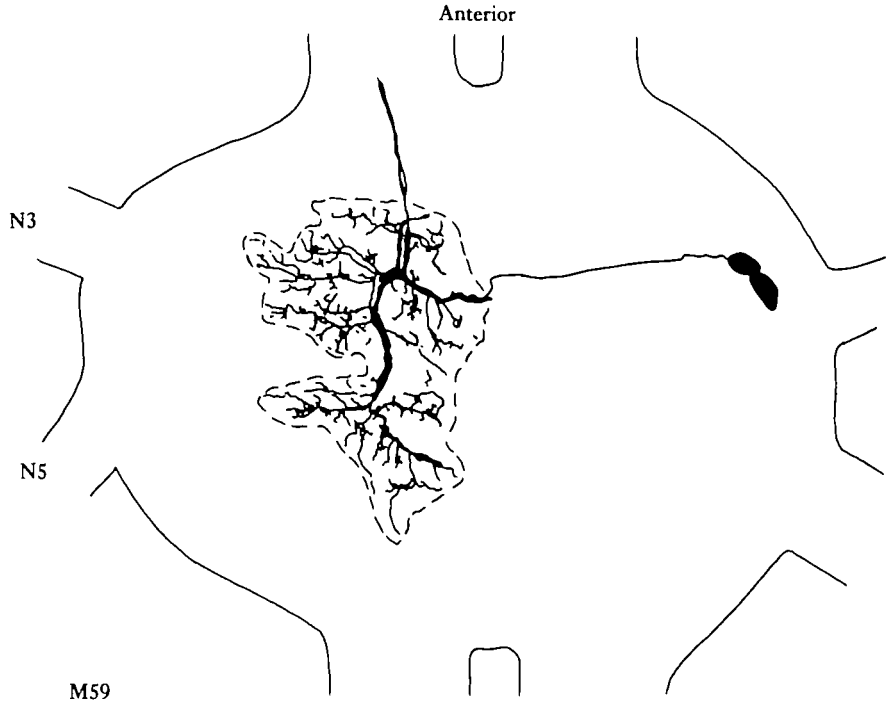

Fig. 14. Reconstruction from photomicrographs of the projections of M59 (intersegmental muscle) motor neurones to the mesothoracic ganglion. This muscle is supplied by a branch of N1 and the axons enter the ganglion close to those of M81. Two cells are stained; their endings are dorsally located within the area enclosed by the dashed line. (3% cobalt chloride for 20 h.)

The response of the motor neurones to electrical stimulation of the hair plates

Both M99 neurones responded to stimulation of the ipsilateral hair plates with a depolarizing synaptic potential, which could give rise to a spike. The amplitude of the EPSP was increased by passing hyperpolarizing current (Fig. 15) which suggests that it is chemical. Increasing either the voltage (Fig. 16A) or the duration of the stimulus increased the size of the EPSP. It is likely that the stronger stimuli stimulated more axons and hence recruited more synapses on the motor neurone. The EPSP followed faithfully at stimulation frequencies of up to 200 Hz; above 30 Hz the EPSPs summated (Fig. 16B). There was no sign of facilitation or habituation.

The latency of the response was extremely short: 4·2 ± 0·44 ms (mean ± S.E.). The extracellular record of activity in the axons of N1C, made near the junction of N1D, showed that the time taken for the axons to conduct to this point was 2·1 ms. Since this distance is three-quarters of that to the ganglion, the expected time of arrival of the axonal impulse in the ventral association area is 2·8 ms. This leaves 1·4 ms for interneurones to convey the excitation to the dorsally located motor neurones. On anatomical grounds (see above) at least two synapses are needed. Assuming that the delay at insect central synapses is 0·7–1·0 ms (see Pearson, Wong & Fourtner, 1976) the connection is likely to be disynaptic.

The EPSP reached its peak after 6·8 ms and then declined, in a smooth exponential lasting 15–30 ms (Fig. 15).

Stimulation of the contralateral hair plates did not always evoke a synaptic potential.

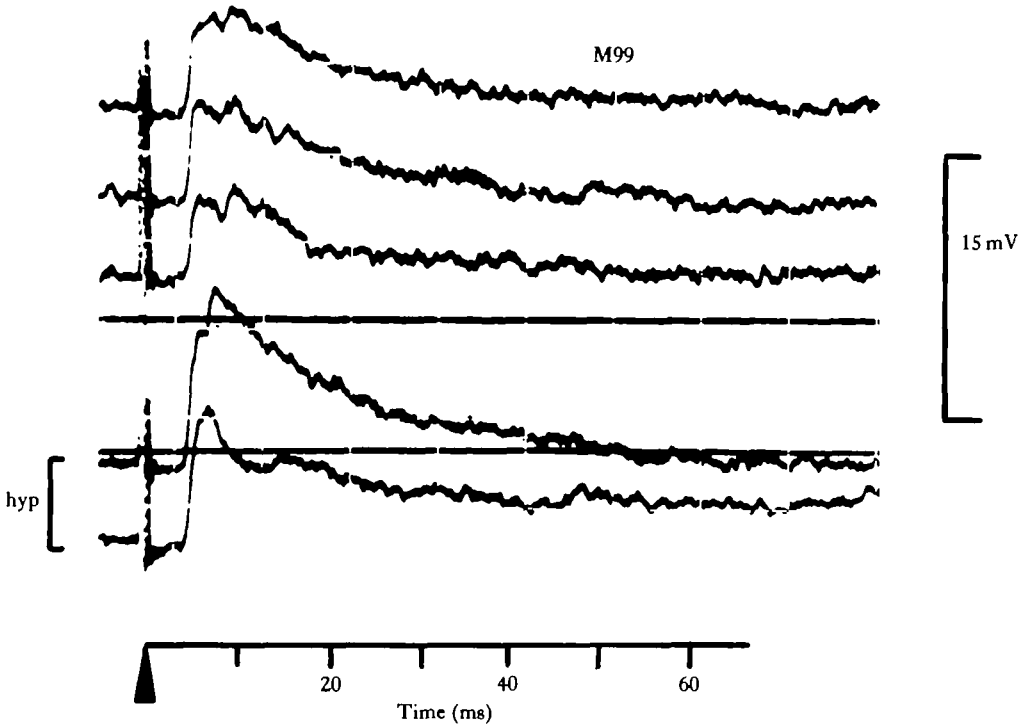

Fig. 15. Response of M99 motor neurones to electrical stimulation of the ipsilateral hair plates. An EPSP is seen after 4 ms. Results of five stimuli are shown; between stimuli the d.c. offset was adjusted. The two lowest responses are to stimuli given during the passage of hyperpolarizing current (hyp) and have a larger amplitude. This suggests that the EPSP is chemical. Compare Fig. 1D of Elliott *et al.* (1982) where the response of another M99 neurone is shown.

In one cell, low frequency stimulation evoked a slow, depolarizing potential that could lead to spikes. The rising phase usually appeared stepped, suggesting that this was the product of several parallel pathways. The latency to the onset was 30 ms and that to the peak was 50 ms.

Two kinds of synaptic response to stimulation of the ipsilateral hair plates were found in the motor neurones of M90. In two of the large neurones with posteriorly located cell bodies (those shown at '*B*' and '*C*' in Fig. 8) there was an EPSP after a latency of $8{\cdot}4 \pm 0{\cdot}35$ ms (mean ±S.E.) (Fig. 17A). As with the M99 EPSP, this EPSP increased with stimulus amplitude and followed at frequencies of up to more than 200 Hz, summating at over 30 Hz (Figs 17B, 18). This EPSP often gave rise to spikes. Since it was enhanced by passing hyperpolarizing current, it appears to be chemically mediated.

The second kind of synaptic response seen in M90 motor neurones was a long latency EPSP, seen in the third large ('*D*') and the small ('slow') cells with posteriorly located cell bodies. The latency to this potential was $16{\cdot}8 \pm 1{\cdot}2$ ms. The potential was long lasting (approx. 80 ms) (Fig. 19), and could give rise to a barrage of spikes in the motor neurone.

The response of the cell '*A*' – with the forward cell body and less extensive branching – was not recorded.

One M85 motor neurone also received a short (8 ms) latency synaptic potential,

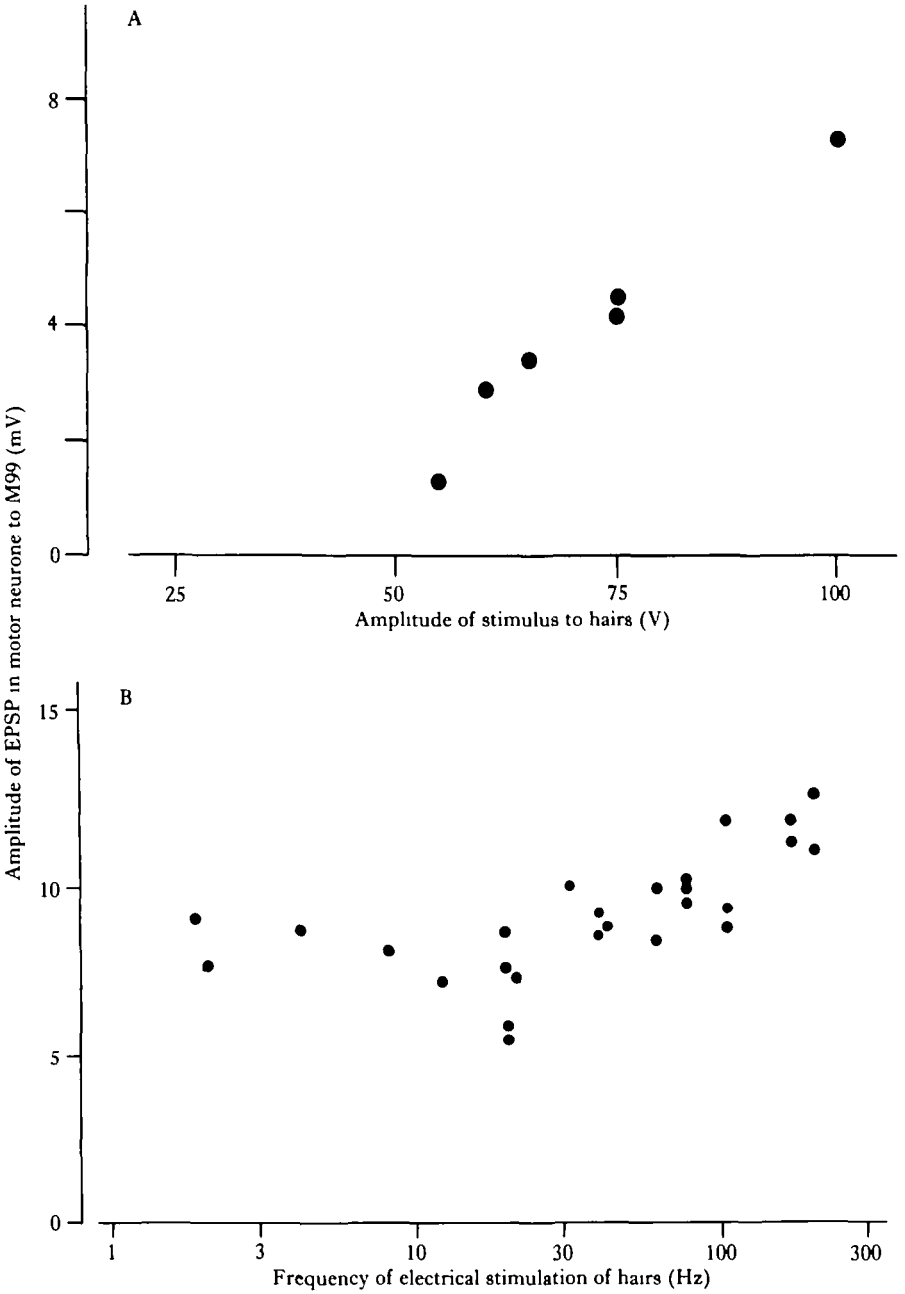

Fig. 16. (A) Increasing size of the EPSP in M99 motor neurone with stimulus voltage. Mean of six stimuli at 1·7 Hz. (B) The amplitude of the EPSP in M99 motor neurone as a function of the frequency of electrical stimulation of the hair plates. Bursts of stimuli were given and the amplitude of the third or fourth EPSP above the resting potential measured.

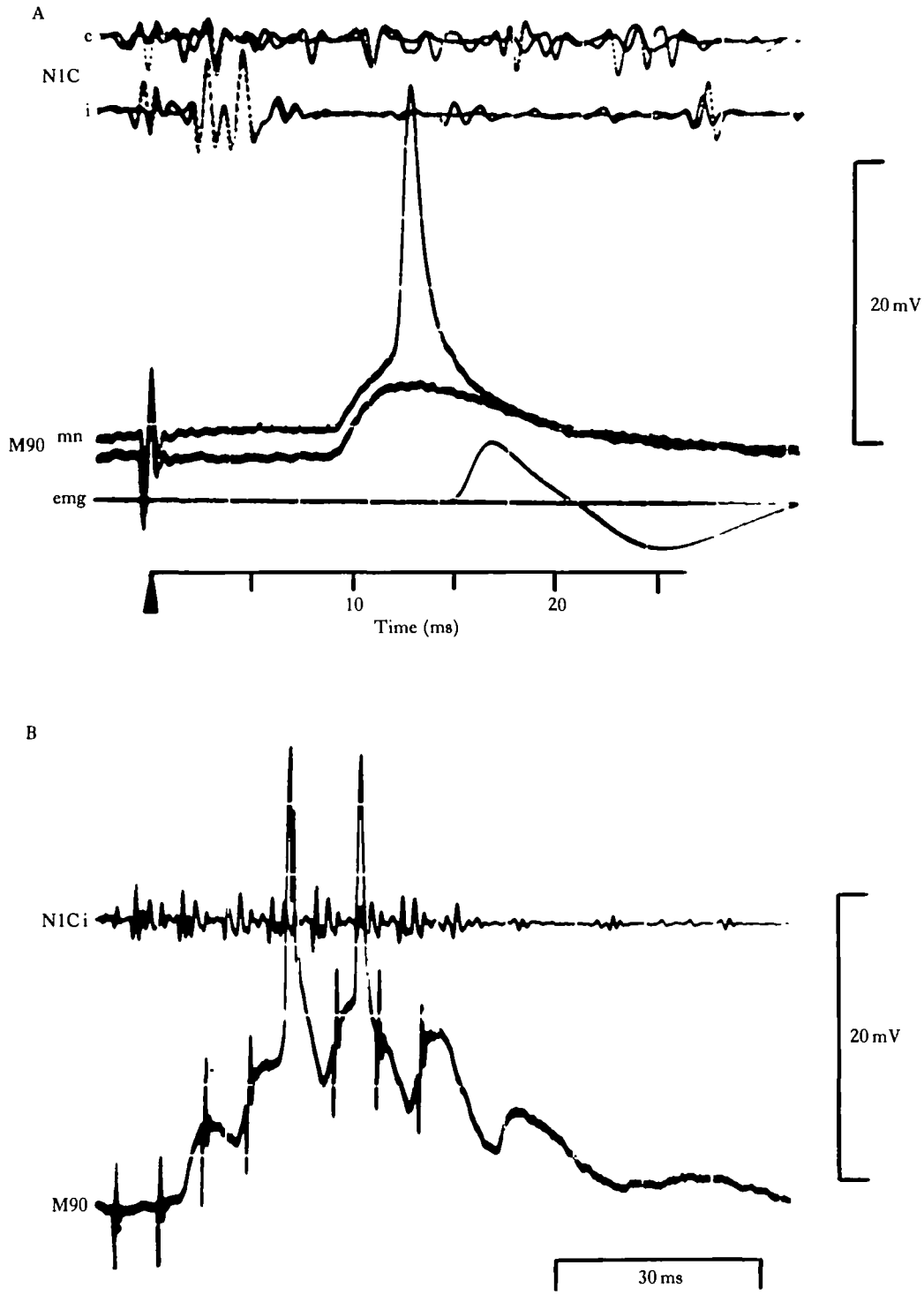

Fig. 17. The response of M90 motor neurone '*B*' to electrical stimulation of the ipsilateral hair plates, recorded intracellularly. Also shown are *en passant* hook electrode recordings from the ipsilateral (i) and contralateral (c) N1C. (A) Two individual shocks both elicit EPSPs after 10 ms. In one, the motor neurone is already somewhat depolarized by other synaptic input and then the EPSP evokes an action potential, which is followed by an EJP in the muscle. (B) Repetitive stimulation at 160 Hz leads to summation of the PSP.

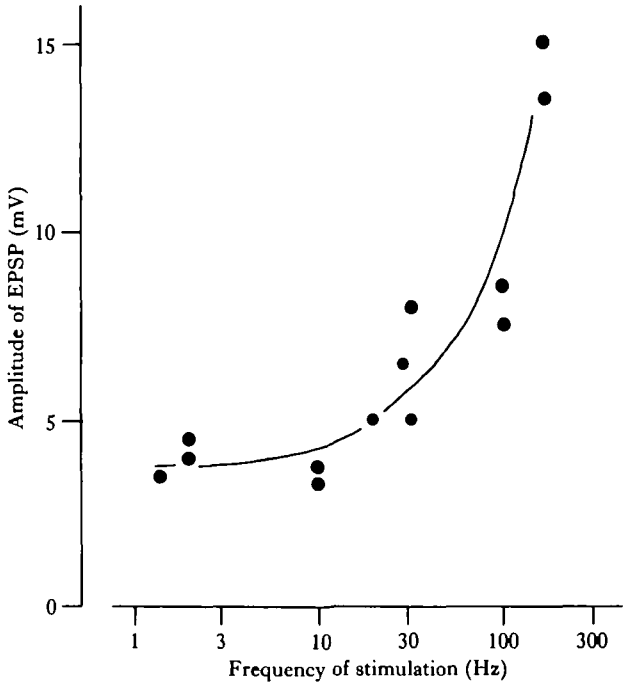

Fig. 18. The amplitude of the EPSP in the M90 motor neurone '*B*' as a function of the frequency of electrical stimulation of the hair plates. Bursts of stimuli were given and the amplitude of the third or fourth EPSP above the resting potential measured.

which could give rise to spikes when the cell was depolarized, following the electrical stimulation of the ipsilateral hair plates.

The latency between spikes recorded intracellularly in the integrating segment of M85, M90, or M99 motor neurone and the EJP in the appropriate muscle was 3–4 ms (Fig. 17A). The delay between the arrival of the nerve impulse in the muscle and the EJP was 1–1·5 ms.

DISCUSSION

The mechanical and electrical properties of the hairs

The measurement of the absolute angular stiffness of the wing hairs of *Gryllus campestris* ($5{\cdot}5 \times 10^{-6}$ Nm rad^{-1}) is to my knowledge the first direct measurement of the static mechanical properties of any insect hairs. The angular stiffness (k) may, however, be estimated from dynamic measurements of the resonant frequency (F_o) and moment of inertia (I) of the hairs using the formula:

$$k = (2\pi F_o)^2 I$$

(Fletcher, 1978). The measurements of Tautz (1977) and Gnatzy & Tautz (1980) on the thoracal hairs of *Barathra* caterpillars and cercal filiform hairs of *Gryllus bimaculatus* give angular stiffnesses of 10^{-12} and 10^{-14} Nm rad^{-1} respectively. These hairs are therefore easier to bend than those of the wings of *Gryllus campestris*. (The moment of inertia includes a contribution from the boundary layer of air, calculated

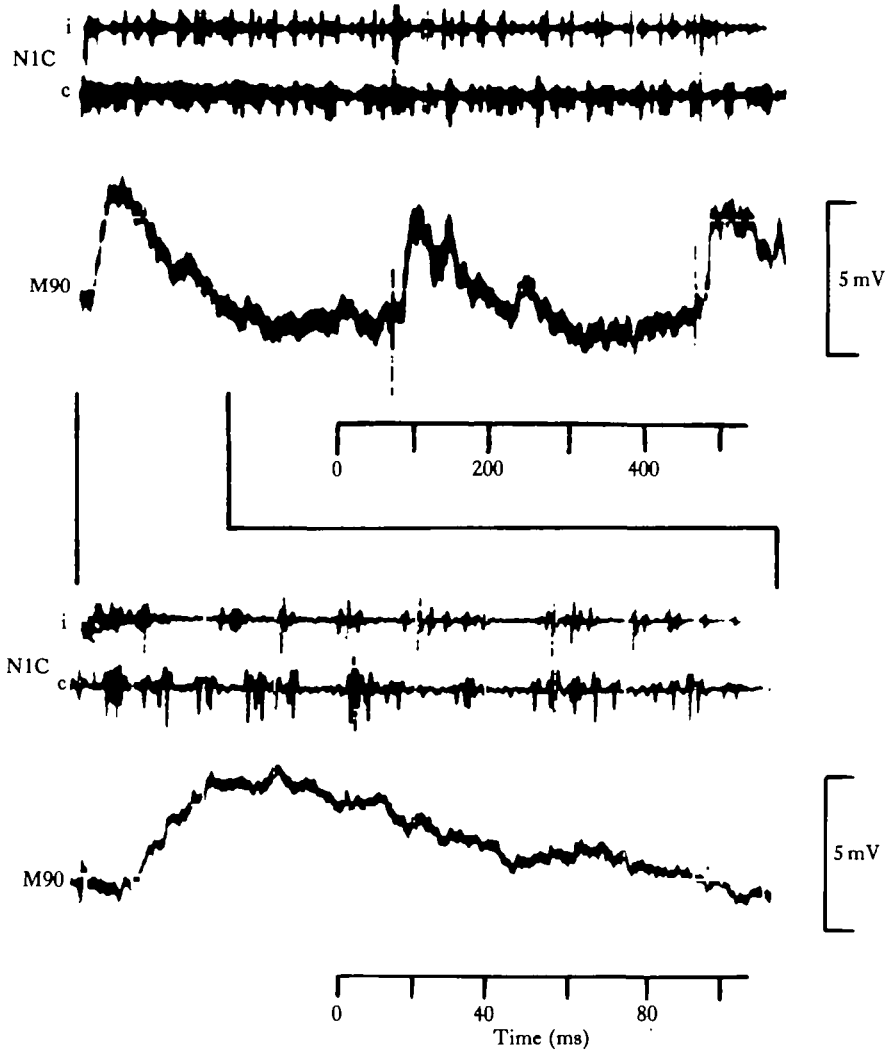

Fig. 19. The response of M90 motor neurone '*D*' to electrical stimulation of the ipsilateral hair plates, recorded intracellularly. Also shown are *en passant* hook electrode recordings from the ipsilateral (i) and contralateral (c) N1C. The upper record shows the response to three shocks at 2·5 Hz. Each stimulus gives rise to a long-lasting EPSP after a latency of 17 ms. Part of the record is shown on an expanded scale below.

according to Fletcher's method, 1978.) Mechanosensory cuticular hairs in crayfish have an angular stiffness of 2×10^{-9} Nm rad^{-1} (Wiese, 1976).

In order that the viscous drag of the air movements during air-borne vibrations should be able to deflect hairs it is necessary that they have a low stiffness – this is clearly true of the thoracal and cercal hairs, mentioned above. Because the density of water is higher than that of air, the hairs on crayfish can be much stiffer than insect filiform hairs and yet function effectively as detectors of low frequency vibrations. But it would seem unlikely that the wing hairs of *Gryllus campestris*, whose stiffness is some six orders of magnitude greater, will be deflected as a result of viscous drag.

This is an important consideration, because though the hairs in the plates between

the wings will bend as the wings rub together during stridulation, the two other ('outer') hair plates (those on the upper surface of the right wing and lower surface of the left wing) cannot be bent by direct action, but only by air movements. It is possible, following Fletcher (1978), to use the stiffness to calculate the expected deflection of the hair due to viscous drag; this is in the order of 0·1°. Indeed the deflection will even be less than this, because Fletcher's (1978) calculation does not take into account a boundary layer of approximately 100 μm (half the length of the hairs) which will reduce the viscous drag. This deflection is well below the neural threshold of the hairs ($\geq$3°, see Fig. 4). For the hairs in the upper hair plates, which are only half the length of those in the lower hair plates (Elliott *et al.* 1982), the viscous drag will be even less. No deflection of the hairs was seen when air from a pipette was blown at them. Thus, the measurement of the stiffness of the hairs provides convincing evidence that only the deformation resulting from rubbing of the wings will be sufficient to stimulate the hairs neurally.

When a hair is bent, receptor and action potentials are recorded, as for other insect mechanoreceptors (Wolbarsht, 1960; Guillet, Bernard, Coillot & Callec, 1980; Erler & Thurm, 1981). The negative going receptor potential may be explained by an influx of cations into the dendrite, depolarizing it and so reducing the positive potential in the hair shaft.

Two sorts of action potentials are observed: first in each cycle comes one with a leading negative phase. If there is more than one spike in each cycle, subsequent spikes are of the second type and are seen with positive phase only. They also have a longer duration. Changes in the shape of mechanoreceptor spikes during stimulation are also reported by Guillet *et al.* (1980) and Erler & Thurm (1981). Previously it has been tacitly supposed that the shape of the recorded spikes gives a reliable indication of the course of the ionic currents (see, e.g. the review by Thurm & Küppers, 1980). That this may not be so with sensory structures is shown by the simultaneous intra- and extracellular recordings of Tomita (1956). What is, however, clear from the wing hair recordings shown above (Fig. 3), is that different shapes of spikes do occur and for these different ionic mechanisms must still be provided. One possibility is that there are slow voltage-dependent conductances inactivated by the first spike, which increase the dendritic membrane resistance. This would increase the time constant of the dendritic membrane and so attenuate or even abolish the fast, leading negative phase but leave the slower, positive phase unaltered. A slow increase in the dendritic membrane resistance following current injection into mechanoreceptors on the leg of *Schistocerca* was suggested by Guillet *et al.* (1980). These hypotheses need further investigation.

The threshold of the neural response to sinusoidal mechanical stimulation is 15°. This compares closely with that of bristles in bee hair plates (10–20°, Thurm, 1963), but is two orders of magnitude greater than the threshold of filiform hairs on cerci (Nicklaus, 1965). Normally spikes are only evoked at one phase of the cycle but they may be induced at a second phase by high deflections. In this respect, the sensillae resemble those from other hair plates in bees (Thurm, 1963) and cockroaches (Wong & Pearson, 1976). The threshold to sinusoidal stimulation about the resting position is relatively independent of direction.

The threshold of the cricket wing hairs is relatively unaffected by the frequency of

the imposed stimulus, at least up to 30 Hz. This means that the hairs will respond if they are rhythmically deflected as a result of stridulatory movements, which occur at 30 Hz. Above threshold, however, the gain (spikes cycle^{-1}) does depend on frequency (Fig. 4), being maximal between 1 and 3 Hz. The hair plates are unlikely to provide much input in non-singing crickets, even if the wings do touch, because their response to maintained displacement is very low.

The projection of the hair sensillae to the thoracic ganglia

The axons of the hairs all project to the ventral association area of the mesothoracic ganglion. Such projections are typical of other sensory hairs (Hustert, 1978; Pflüger, Bräunig & Hustert, 1981; Tyrer *et al.* 1979), though these often have projections in the ventral association area of more than one ganglion. The hairs have no projections dorsally, unlike the hair plates at leg joints (Pflüger *et al.* 1981) on the head (Altman & Kien, 1979) and neck (Kien, 1980).

At least some of the hairs in the leg hair plates make monosynaptic connections with motor neurones (Pearson *et al.* 1976) and so can play a direct role in controlling walking. Indeed, the results of Bässler & Wegner (1983) indicate that the generation of normal stick insect walking patterns is based on successive sensory inputs. There is good evidence, however, for central, interneuronal generation of stridulatory patterns (Bentley, 1969; Kutsch & Huber, 1970; Elepfandt, 1980). If interneurones which are part of the pattern generator were directly excited by the afferents then dorsal projections to motor neurones would be unnecessary.

The anatomy and physiology of the motor neurones

The anatomical descriptions have been summarized and discussed above. It remains to stress that, though each muscle is multiply innervated, the motor neurones are not redundant replicas of each other. Each has its own distinct anatomy, innervating a particular part of the muscle. This corresponds with Neville's (1963) demonstration in *Schistocerca* that the five neurones to the dorsal longitudinal muscle all run to different parts of the muscle. Again each motor neurone has its own pattern of synaptic inputs and its own behavioural role (Kutsch, 1969).

The motor neurones to muscle 90 (closer) and 99 (opener) are synaptically excited as a result of the electrical stimulation of the ipsilateral hair plates. Because of the method of stimulation used, axons of sensillae in both hair plates will be excited. The synaptic potential is evoked after a latency of 4–17 ms, depending on the motor neurone. They appear to be chemically mediated and cannot, on anatomical grounds, be monosynaptic. The shorter (4–10 ms) latency EPSPs have a steep rising phase and slow decay, which is characteristic of a single, strong synaptic input. This means that the input comes either from a single presynaptic neurone, or else from a group of highly synchronized neurones. The size of the PSP – up to 8 mV – shows that there must, in either case, be many parallel postsynaptic sites on the motor neurone. In contrast, the EPSPs evoked after a latency of 17 ms have a slow rise as well as fall, which suggests that the excitation comes from several parallel pathways, each with different individual delays.

Each of the ipsilateral EPSPs to M90 and 99 follow reliably up to 200 Hz. Above 30 Hz the PSPs summate, because their duration is 15–20 ms, which is determined

by the time constant of the motor neurone membrane. Since 30 Hz is the frequency of the stridulatory movements, this shows that the physical properties of the motor neurone membranes are adapted to their role.

These EPSPs, because of their reliability, are potential neuronal explanations of the behavioural changes resulting from the removal of the hair plates. This is not a property of the long latency PSP recorded in M99 motor neurones following stimulation of the contralateral hair plates; perhaps this could be part of a grooming response or avoidance movement. The long latency (30 ms) allows time for the brain to be involved or for a peripheral reflex.

Physiological explanations of a behavioural role for the hair plates

The physiological characterization of the hair plates and their relationship with the motor neurones described above was undertaken to provide an explanation of recent behavioural observations (Elliott & Koch, 1983), which showed that the hair plates are important in controlling the wing movements during stridulation; their results may be summarized as follows:

(i) removal of the 'inner' hair plates results in the wings being held further apart during stridulation,

(ii) removal of one inner hair plate results in half the increase in opening when both are removed,

(iii) removal of both 'inner' hair plates also decreases the stability of the opening position,

(iv) removal of the 'outer' hair plates has little effect on wing position.

The last result can be explained by the observation that air movements alone are not sufficient to stimulate the wing hairs. Only the direct rubbing action of the wings will deflect the hairs enough to evoke action potentials. Thus, no change in behaviour can be expected when the outer hairs are removed; this is indeed observed.

The effect of removing the inner hair plates might be mediated as follows. During stridulation, the rubbing action of the wings deforms these hairs sufficiently to evoke action potentials, some in the opening stroke and others in the closing stroke. Then the excitation will be conveyed to the mesothoracic ganglion and produce EPSPs in the motor neurones to M85, the wing-folding muscle. This muscle is tonically active in the calling song (Kutsch, 1969) and the shape of the EJPs suggests that this is a slow muscle. If now the hairs are removed, then the EPSPs will no longer occur in the motor neurones, the firing rate and tension will decline and so the wing will not be held so close to the body: i.e. the wings will be held further apart. Removal of one hair plate will only affect the position of the ipsilateral wing and so should produce half the change in wing position caused by removal of both hair plates; as is in fact seen (Elliott & Koch, 1983). Because M85 is a tonic muscle, the hypothesis predicts that the effect should be a 'd.c. shift'; the closing position and position between chirps should be affected as much as the opening position and this is indeed the case (Elliott & Koch, 1983). Again it would be possible to explain the stabilizing effect of the hair plates; opening the wings too far would increase the stimulus (and hence the amplitude of the EPSP) because the hairs are close to the edge of the wing. This hypothesis assumes that the EPSP in M85 resembles those in M99 and M90 (opener and closer) and does not habituate to the repeated stimulation that would occur in singing. Electromyograms

from M85 before and after removal of the hair plates would provide an excellent test for this hypothesis.

The roles of the EPSP in M90 (closer) and M99 (opener) in the control of wing position are not so readily explained. Part of the problem is that stimulating the hair plates evokes EPSPs in both the antagonistic muscles, albeit after different latencies. A singing male with all hairs intact holds his wings further apart when singing in the inverted (left over right) than in the normal (right over left) orientation (Elliott & Koch, 1983). Each wing has two hair plates, one ('inner') stimulated only in normal singing, the other ('outer') only in inverted singing and so the difference in wing position indicates that inner and outer hair plates signal in opposite senses. It could be, then, that the axons of the inner hair plates excite M90 (closer) motor neurones and those of the outer hair plates those of M99 (opener). This could be tested by stimulating the upper and lower hair plates separately, using a mechanical stimulator.

On this hypothesis, in normal stridulation (right over left), the inner hair plates are stimulated about halfway through the closing stroke. These excite the closer motor neurones (e.g. M90) after a delay of 8 or 17 ms, depending on the neurone. This would then advance the time at which an action potential is produced, preventing excessive opening. If the hairs are removed, the action potential in the closer is delayed, and the wings can be opened too far. If the wings are inverted, so that the outer hair plates are now stimulated, then an extra EPSP is evoked in the opener motor neurones (M99) and no hair plate EPSP is found in the closer (e.g. M90) so delaying the action potential. Both these effects serve to produce an opening larger than that seen in normal stridulation.

It seems, then, that the cricket has two parallel pathways which control wing movements during stridulation: one involving a tonic muscle, M85, and one whose action is *via* phasic muscles, the openers and closers. In addition, there may be other effects of the hair plates – for example, on central pattern generating neurones – which are not revealed by recording from the motor neurones in quiescent preparations.

Neither of these mechanisms for the control of wing position resemble the models put forward by Wendler (1964) and Wong & Pearson (1976) to explain the control of leg position by hair plates. In these models, the hair plates are activated when full retraction occurs, causing a switch to protraction. Thus the hair plates prevent excessive retraction. Such a mechanism cannot work in cricket stridulation, because the time for the reflex (13 ms at least) is long compared with the duration of the stridulatory strokes.

I should like to take this opportunity of thanking all my colleagues in Seewiesen whose advice and help have contributed to this project. I am particularly grateful to Professor F. Huber for his many constructive suggestions and financial support through the Max Planck Gesellschaft. I am also pleased to be able to thank Karen Meyer for much practical help and Monika Kasparek, Koos de Kramer, Uwe Koch and Dirk Korschenhausen for their assistance.

REFERENCES

ALTMAN, J. S. & KIEN, J. (1979). Suboesophageal neurons involved in head movements and feeding in locusts. *Proc. R. Soc. B* **205**, 209–227.

ALTMAN, J. S. & TYRER, N. M. (1977). The locust wing hinge stretch receptors. I. Primary sensory neurones with enormous central arborizations. *J. comp. Neurol.* **172**, 409–430.

ALTMAN, J. S. & TYRER, N. M. (1980). Filling selected neurons with cobalt through cut axons. In *Neuroanatomical Techniques. Insect Nervous System*, (eds N. J. Strausfeld & T. A. Miller), pp. 373–402. New York: Springer-Verlag.

BACON, J. P. & ALTMAN, J. S. (1977). A silver intensification method for cobalt-filled neurones in wholemount preparations. *Brain Res.* **138**, 359–363.

BÄSSLER, U. & WEGNER, U. (1983). Motor output of the denervated thoracic ventral nerve cord in the stick insect *Carausius morosus*. *J. exp. Biol.* **105**, 127–145.

BENTLEY, D. (1969). Intracellular activity in cricket neurons during generation of song patterns. *Z. vergl. Physiol.* **62**, 267–283.

BISHOP, C. A. & O'SHEA, M. (1982). Neuropeptide proctolin (H-Arg-Try-Leu-Pro-Thr-OH): immunocytochemical mapping of neurons in the central nervous system of the cockroach. *J. comp. Neur.* **207**, 223–238.

BURROWS, M. (1973). The morphology of an elevator and a depressor motoneuron of the hindwing of a locust. *J. comp. Physiol.* **83**, 165–178.

CAMHI, J. M. (1969). Locust wing receptors. I. Transducer mechanics and sensory response. *J. exp. Biol.* **50**, 335–348.

COMSTOCK, J. H. & NEEDHAM, J. G. (1899). The wings of insects. Chapter IV: The specialization of wings by addition. V. The tracheation of the wings of Orthoptera. *Am. Nat.* **33**, 573–582.

ELEPFANDT, A. (1980). Morphology and output couplings of wing muscle motor neurones in the field cricket (Gryllidae, Orthoptera). *Zool. Jb. (Physiol.)* **84**, 26–45.

ELLIOTT, C. J. H. & KOCH, U. T. (1983). Sensory feedback stabilizing reliable stridulation in the field cricket *Gryllus campestris* L. *Anim. Behav.* **31**, 887–901.

ELLIOTT, C. J. H., KOCH, U. T., SCHÄFFNER, K.-H. & HUBER, F. (1982). Wing movements during cricket stridulation are affected by mechanosensory input from wing hair plates. *Naturwissenschaften* **69**, 288–289.

ERLER, G. & THURM, U. (1981). Dendritic impulse initiation in an epithelial sensory neuron. *J. comp. Physiol.* **142**, 237–249.

FLETCHER, N. H. (1978). Acoustical response of hair receptors in insects. *J. comp. Physiol.* **127**, 185–189.

GALLYAS, F., LÉNÁRD, L. & LAZAR, G. (1978). Improvement of cobalt-transport in axons by complexing agents. *Neurosci. Lett.* **9**, 213–216.

GNATZY, W. & TAUTZ, J. (1980). Ultrastructure and mechanical properties of an insect mechanoreceptor: stimulus transmitting structures and sensory apparatus of the cercal filiform hairs of *Gryllus*. *Cell Tiss. Res.* **213**, 441–463.

GUILLET, J. C., BERNARD, J., COILLOT, J. P. & CALLEC, J. J. (1980). Electrical properties of the dendrite in an insect mechanoreceptor: effects of antidromic or direct electrical stimulation. *J. Insect Physiol.* **26**, 755–762.

HUBER, F. (1962). Central nervous control of sound production in crickets and some speculations on its evolution. *Evolution* **16**, 429–442.

HUSTERT, R. (1978). Segmental and interganglionic projections from primary fibers of insect mechanoreceptors. *Cell Tiss. Res.* **194**, 337–351.

KAISSLING, K.-E. & THORSON, J. (1980). Insect olfactory sensilla: structural, chemical and electrical aspects of the functional organization. In *Receptors for Neurotransmitters, Hormones and Pheromones in Insects*, (eds D. B. Sattelle, L. M. Hall & J. G. Hildebrand). Elsevier/North Holland Press.

KEILBACH, R. (1935). Über asymmetrische Flügellage bei Insekten und ihre Beziehungen zu anderen Asymmetrien. *Z. Morph. Ökol. Tiere* **29**, 1–44.

KIEN, J. (1980). Morphology of locust neck muscle motoneurons and some of their inputs. *J. comp. Physiol.* **140**, 321–336.

KUTSCH, W. (1969). Neuromuskuläre Aktivität bei verschiedenen Verhaltenswiesen von drei Grillenarten. *Z. vergl. Physiol.* **63**, 335–378.

KUTSCH, W. & HUBER, F. (1970). Zentrale versus periphere Kontrolle des Gesanges von Grillen (*Gryllus campestris*). *Z. vergl. Physiol.* **67**, 140–159.

KUTSCH, W. & USHERWOOD, P. N. R. (1970). Studies of the innervation and electrical activity of flight muscles in the locust *Schistocerca gregaria*. *J. exp. Biol.* **52**, 299–312.

MÖSS, D. (1971). Sinnesorgane im Bereich des Flügels der Feldgrille (*Gryllus campestris* L.) und ihre Bedeutung fur die Kontrolle der Singbewegung und die Einstellung der Flügellage. *Z. vergl. Physiol.* **73**, 53–83.

NEVILLE, A. C. (1963). Motor unit distribution of the dorsal longitudinal flight muscles in locusts. *J. exp. Biol.* **40**, 123–136.

NICKLAUS, R. (1965). Die Erregung einzelner Fadenhaare von *Periplaneta americana* in Abhängigkeit von der Grösse und Richtung der Auslenkung. *Z. vergl. Physiol.* **50**, 331–362.

PEARSON, K. G. & FOURTNER, C. R. (1975). Nonspiking interneurons in the walking system of the cockroach. *J. Neurophysiol.* **38**, 33–52.

PEARSON, K. G., WONG, R. K. S. & FOURTNER, C. R. (1976). Connexions between hair plate afferents and motoneurones in the cockroach leg. *J. exp. Biol.* **64**, 251–266.

PFLÜGER, H. J., BRÄUNIG, P. & HUSTERT, R. (1981). Distribution and specific central projections of mechanoreceptors in the thorax and proximal leg joints of locusts. II. The external mechanoreceptors: hair plates and tactile hairs. *Cell Tiss. Res.* **216**, 79–96.

REGEN, J. (1903). Neue Beobachtungen über die Stridulationsorgane der Saltatoren Orthopteren. *Arb. zool. Inst. Univ. Wien* **14**, 359–422.

STÄRK, A. A. (1958). Untersuchungen am Lautorgan einiger Grillen- und Laubheuschrecken- Arten, zugleich ein Beitrag zum Rechts-Links-Problem. *Zool. Jb. (Anat.)* **77**, 9–50.

STEWART, W. W. (1978). Functional connections between cells as revealed by dye-coupling with a highly fluorescent Naphthalimide tracer. *Cell* **14**, 741–759.

TAUTZ, J. (1977). Reception of medium vibration by thoracal hairs of caterpillars of *Barathra brassicae* L. (Lepidoptera, Noctuidae). I. Mechanical properties of the receptor hairs. *J. comp. Physiol.* **118**, 13–31.

THURM, U. (1963). Die Beziehungen zwischen mechanischen Reizgrössen und stationaren Erregungzuständen bei Borstenfeld-sensillen von Bienen. *Z. vergl. Physiol.* **46**, 351–382.

THURM, U. & KÜPPERS, J. (1980). Epithelial physiology of insect sensilla. In *Insect Biology in the Future*, (eds M. Locke & D. Smith). New York: Academic Press.

TOMITA, T. (1956). The nature of action potentials in the lateral eye of the horseshoe crab as revealed by simultaneous intra- and extracellular recording. *Jap. J. Physiol.* **6**, 327–340.

TYRER, N. M. & ALTMAN, J. S. (1974). Motor and sensory flight neurones in a locust demonstrated using cobalt chloride. *J. comp. Neur.* **157**, 117–138.

TYRER, N. M., BACON, J. P. & DAVIES, C. A. (1979). Sensory projections from the wind-sensitive head hairs of the locust *Schistocerca gregaria*. Distribution in the central nervous system. *Cell Tiss. Res.* **203**, 79–92.

TYRER, N. M. & GREGORY, G. E. (1982). A guide to the neuroanatomy of locust suboesophageal and thoracic ganglia. *Phil. Trans. R. Soc. Ser. B.* **297**, 91–123.

VOSS, F. (1904). Über den Thorax von *Gryllus campestris*. I. Das Skelett. *Z. wiss. Zool.* **78**, 267–351.

WENDLER, G. (1964). Laufen und Stehen der Stabheuschrecke *Carausius morosus*: Sinnesborstenfelder als Glieder von Regelskreisen. *Z. vergl. Physiol.* **48**, 198–250.

WIESE, K. (1976). Mechanoreceptors for nearfield water displacements in crayfish. *J. Neurophysiol.* **39**, 816–833.

WOHLERS, D. W. & HUBER, F. (1978). Intracellular recording and staining of cricket auditory interneurons (*Gryllus campestris* L., *Gryllus bimaculatus* De Geer). *J. comp. Physiol.* **127**, 11–28.

WOLBARSHT, M. L. (1960). Electrical characteristics of insect mechanoreceptors. *J. gen. Physiol.* **44**, 105–122.

WONG, R. K. S. & PEARSON, K. G. (1976). Properties of the trochanteral hair plate and its function in the control of walking in the cockroach. *J. exp. Biol.* **64**, 233–249.

ZAWARZIN, A. (1924). Histologische Studien über Insekten. VI. Zur Morphologie der Nervenzentren. Das Bauchmark der Insekten. *Z. wiss. Zool.* **122**, 323–424.